6th International Conference on CFD in the Oil & Gas, Metallurgical and Process Industries *CFD2008-078*
SINTEF / NTNU, Trondheim, Norway
10–12 June 2008

A COMPUTATIONAL STUDY OF THE COALESCENCE PROCESS BETWEEN A DROP AND AN INTERFACE IN AN ELECTRIC FIELD

Knut Erik TEIGEN,[1*] **Svend Tollak MUNKEJORD,**[2] **Erik BJØRKLUND**[3]

[1] NTNU, Department of Energy and Process Engineering, 7491 Trondheim, Norway
[2] SINTEF Energy Research, Energy Processes, 7465 Trondheim, Norway
[3] Aibel AS, 1375 Billingstad, Norway
[*] E-mail: knutert@gmail.com

ABSTRACT

The coalescence process between a drop and an interface may not be instantaneous, but result in the creation of a smaller secondary drop. This process may be repeated several times before the coalescence is complete. Experiments have shown that an electric field can suppress this phenomenon and give coalescence in a single stage. In this paper, the influence of an electric field on the partial coalescence process is studied using numerical simulations. The results show that higher electric Bond numbers reduce the time from pinch-off of a secondary drop to recoalescence, and eventually give single-staged coalescence. A single-stage coalescence event is presented in detail, and the mechanism producing it discussed. The results support arguments from the literature that single-staged coalescence is caused by an increased downward momentum due to electrostatic attraction.

Keywords: Coalescence, electrocoalescence, electrohydrodynamics, level-set method, ghost-fluid method

NOMENCLATURE

δ	Dirac delta function
Ψ	Electric potential [V]
Γ	Interface
κ	Curvature [m^{-1}]
ϕ	Level-set function
μ	Dynamic viscosity [$\mathrm{Pa}\cdot\mathrm{s}$]
$\mu^\star$	Viscosity ratio
ε	Relative permittivity
ε_0	Vacuum permittivity ($= 8.85 \times 10^{-12}\,\mathrm{F/m}$)
$\varepsilon^\star$	Permittivity ratio
ρ	Density [$\mathrm{kg/m}^3$]
$\rho^\star$	Density ratio
σ	Interfacial tension [$\mathrm{N/m}^2$]
τ	Pseudo-time
τ_2	Time from pinch-off to recoalescence
$\boldsymbol{M}$	Maxwell stress tensor [$\mathrm{N/m}^2$]
$\boldsymbol{a}$	Temporary vector field [$\mathrm{m/s}^2$]
$\boldsymbol{e}$	Electric field [V/m]
$\boldsymbol{F}$	Strength of surface force [$\mathrm{N/m}^2$]
$\boldsymbol{f}$	Arbitrary vector field
$\boldsymbol{g}$	Gravitational acceleration [$\mathrm{m/s}^2$]
$\boldsymbol{n}$	Unit normal vector
$\boldsymbol{t}$	Unit tangential vector
$\boldsymbol{u}$	Velocity [m/s]
$\boldsymbol{X}$	Interface parametrization [m]
$\boldsymbol{x}$	Spatial position [m]
$\hat{\boldsymbol{F}}$	Surface force [$\mathrm{N/m}^3$]
a	x-aligned semi-axis of ellipse [m]
b	y-aligned semi-axis of ellipse [m]
D	Diameter [m]
e	Ellipse eccentricity
p	Pressure [Pa]
S	Sign function
t	Time [s]
t_{ic}	Inertio-capillary time
Be	Electric Bond number ($= \varepsilon_1\varepsilon_0 D E_0^2/\sigma$)
Bo	Bond number ($= \lvert\rho_1 - \rho_2\rvert g D^2/\sigma$)
Oh	Ohnesorge number ($= \mu_1/\sqrt{\rho_1\sigma D}$)

INTRODUCTION

Electric fields are currently being employed to speed up the separation of water from oil during oil production from offshore wells. An electric field increases the coalescence rate between water drops which again enhances the settling process. Numerical calculations may give additional insight into the fundamental processes occurring in an electrocoalescer, and thereby help to optimize the separation process.

The partial coalescence phenomenon was made widely known by Charles and Mason (1960a) and Charles and Mason (1960b). They attributed the phenomenon to a static Rayleigh-Plateau instability, and gave a criterion for partial coalescence based on the viscosity ratio. However, in Blanchette and Bigioni (2006), it was demonstrated that the Rayleigh-Plateau instability could not be the cause of the instability, and instead proposed the convergence of capillary waves on the tip of the droplet as the dominating mechanism. A detailed study of the propagation of these capillary waves was made in Gilet *et al.* (2007), and it was concluded that other viscous mechanisms also play an important role in the process.

In Thoroddsen and Takehara (2000), partial coalescence was observed in a system with a viscosity ratio much higher than the criterion stated in Charles and Mason (1960b). Blanchette and Bigioni tried to give a criterion based on the Ohnesorge number and the Bond number, and found that for low Bond numbers, i.e. for drops with negligible gravitational effects, the critical Ohnesorge number was approximately 0.026. Yue *et al.* (2006) made an extensive parameter study using numerical simulations, and found an expression for the critical Ohnesorge number based on the viscosity ratio. However, they did not consider larger Bond numbers, so a universal criterion for the occurrence of partial coalescence remains elusive.

The influence of electric fields on the partial coalescence phenomenon was discussed briefly in Charles and Mason (1960b). It was observed that the rest time of the drop decreased when an electric field was applied. Also, above a critical field strength, the drop was found to coalesce with the interface in a single stage. In Allan and Mason (1961), the influence of electric fields was studied in more detail. They proposed that single-stage coalescence was a result of an additional downward momentum of the water column due to electrostatic attraction, leading to a faster emptying of the drop.

The present work investigates the influence of an electric field on the partial coalescence process using numerical simulations. First, the governing equations and numerical methods are presented. These are then validated by comparison with experimental and theoretical results. Finally, calculations of the partial coalescence process with applied electric fields are presented and discussed.

GOVERNING EQUATIONS AND NUMERICAL METHODS

The numerical method used for the calculations is described in detail in Bjørklund (2008) and Hansen (2005), and will only be briefly reviewed here. The full Navier–Stokes equations are solved in each phase, and the interface between the two phases is captured using the level-set method. The ghost-fluid method is used to treat discontinuities across the interface in a sharp manner. To account for electric forces, a Poisson equation is solved for the electric potential, which is then used to calculate the Maxwell stress tensor.

Flow equations

The flow is governed by the incompressible Navier–Stokes equations, with added terms for surface tension forces and electric forces:

$$\begin{aligned}\rho\left(\frac{\partial \boldsymbol{u}}{\partial t}+(\boldsymbol{u}\cdot\nabla)\boldsymbol{u}\right) &= -\nabla p+\nabla\cdot[\mu(\nabla\boldsymbol{u}+\nabla\boldsymbol{u}^T)]+\rho\boldsymbol{g}\\ &\quad +\hat{\boldsymbol{F}}+\nabla\cdot\boldsymbol{M},\\ \nabla\cdot\boldsymbol{u} &= 0.\end{aligned} \tag{1}$$

The effect of an interface, Γ, in the domain results in a singular surface force which can be expressed by

$$\hat{\boldsymbol{F}}(\boldsymbol{x},t)=\int_{\Gamma(t)}\boldsymbol{F}(s,t)\delta(\boldsymbol{x}-\boldsymbol{X}(s,t))\mathrm{d}s, \tag{2}$$

where s is the arc-length, $\boldsymbol{X}(s,t)$ is the parametrization of the interface, $\boldsymbol{x}$ is the spatial position and δ is the Dirac delta function. $\boldsymbol{F}$ is given by

$$\boldsymbol{F}=\sigma\kappa\boldsymbol{n}. \tag{3}$$

Here, σ is the interfacial tension, κ the curvature and $\boldsymbol{n}$ is the outward pointing unit normal vector.

In this work, all equations are solved in an axisymmetric geometry, so that the divergence operator and Laplacian operator become

$$\nabla\cdot\boldsymbol{f}=\frac{1}{x}\frac{\partial}{\partial x}(xf_x)+\frac{\partial f_y}{\partial x}=\frac{\partial f_x}{\partial x}+\frac{\partial f_y}{\partial y}+\frac{f_x}{x}, \tag{4}$$

$$\nabla\cdot(\nabla\boldsymbol{f})=\frac{1}{x}\frac{\partial}{\partial x}\left(x\frac{\partial\boldsymbol{f}}{\partial x}\right)+\frac{\partial^2\boldsymbol{f}}{\partial y^2}=\frac{\partial^2\boldsymbol{f}}{\partial x^2}+\frac{\partial^2\boldsymbol{f}}{\partial y^2}+\frac{1}{x}\frac{\partial\boldsymbol{f}}{\partial x} \tag{5}$$

where the subscripts indicate the component, and not the partial derivative of the vector $\boldsymbol{f}$. In addition to the above Laplace operator, one has to add $-f_x/x^2$ to the viscous term in the x–momentum equation.

Electric forces

We assume perfect dielectric materials with no free charges. In Allan and Mason (1961), it was concluded

that the ionic strength of the aqueous solution had little influence on the coalescence process. Furthermore, Brown and Hanson (1965) found that it is the electric field at the interface, rather than the charge it carries, that is dominating the process.

With these assumptions, the electric potential, Ψ, can be calculated from the following Laplace equation:

$$\nabla\cdot(\varepsilon\varepsilon_0\nabla\Psi) = 0, \tag{6}$$

The electric field can then be calculated as

$$\boldsymbol{e} = -\nabla\Psi, \tag{7}$$

and the Maxwell stress tensor as

$$\boldsymbol{M} = \varepsilon\varepsilon_0\left[\boldsymbol{ee} - \frac{1}{2}(\boldsymbol{e}\cdot\boldsymbol{e})\boldsymbol{I}\right], \tag{8}$$

where $\boldsymbol{I}$ is the identity tensor. With the above assumptions, $\nabla\cdot\boldsymbol{M} = \boldsymbol{0}$ everywhere except at the interface.

Interface capturing

The interface is captured using the level-set method (Sussman *et al.* (1994); Osher and Fedkiw (2003)). This method allows accurate computation of the evolution of an interface, along with automatic handling of topological changes. The ghost-fluid method (Fedkiw (1999); Kang *et al.* (2000)) is used to take discontinuities across the interface into account. This method handles the jumps in physical properties directly in the numerical stencils, without the need for any smearing of properties.

The interface is defined by the zero level set

$$\Gamma = \{\boldsymbol{x}|\phi(\boldsymbol{x},t) = 0\}, \tag{9}$$

and is evolved by

$$\frac{\partial\phi}{\partial t} + \boldsymbol{u}_{\text{int}}\cdot\nabla\phi = 0. \tag{10}$$

Here, $\boldsymbol{u}_{\text{int}}$ is the velocity on the interface. To be able to solve this equation numerically, the interface velocity is extended off the interface. In Adalsteinsson and Sethian (1999), it was shown that the velocity could be extrapolated orthogonally from the interface by solving

$$\frac{\partial\boldsymbol{u}}{\partial\tau} + S(\phi_0)\boldsymbol{n}\cdot\nabla\boldsymbol{u} = 0, \tag{11}$$

where S is a sign function given by

$$S(\phi) = \frac{\phi}{\sqrt{\phi^2 + 2\Delta x^2}}. \tag{12}$$

Note that this equation is hyperbolic, so it is not necessary to solve it to steady state, since only the information a few grid points away from the interface is relevant.

The standard level-set reinitialization procedure is used to keep the level-set function as a signed distance function throughout the computation. This is accomplished by solving

$$\begin{aligned}\frac{\partial\phi}{\partial\tau} + S(\phi_0)(|\nabla\phi| - 1) &= 0,\\ \phi(\boldsymbol{x},0) &= \phi_0(\boldsymbol{x}).\end{aligned} \tag{13}$$

Reinitialization is performed every second time step.

The ghost-fluid method is used to handle the discontinuities across the interface in a sharp manner. This method requires jump conditions, which are relations between the physical quantities on each side of the interface. In the following, the interfacial jump is denoted by $[x] = x^+ - x^-$, where x^+ is the interfacial value on the side of the interface where ϕ is positive, and x^- is on the other side.

The jump in the velocity gradient is

$$[\mu\nabla\boldsymbol{u}] = [\mu]\boldsymbol{n}\cdot\nabla(\boldsymbol{u}\cdot\boldsymbol{n})\boldsymbol{nn} + [\mu]\boldsymbol{t}\cdot\nabla(\boldsymbol{u}\cdot\boldsymbol{n})\boldsymbol{nt} \tag{14}$$

$$- [\mu]\boldsymbol{t}\cdot\nabla(\boldsymbol{u}\cdot\boldsymbol{n})\boldsymbol{tn} \tag{15}$$

$$+ [\mu]\boldsymbol{t}\cdot\nabla(\boldsymbol{u}\cdot\boldsymbol{t})\boldsymbol{tt}, \tag{16}$$

where $\boldsymbol{t}$ the tangential vector. The jump in the pressure is

$$[p] = 2[\mu]\boldsymbol{n}\cdot\nabla\boldsymbol{u}\cdot\boldsymbol{n} + \boldsymbol{n}\cdot[\boldsymbol{M}]\cdot\boldsymbol{n} + \sigma\kappa\boldsymbol{n}\cdot\boldsymbol{n}, \tag{17}$$

The jump conditions for the electric potential and its gradient are

$$[\Psi] = 0, \tag{18}$$

$$[\varepsilon\varepsilon_0\nabla\Psi\cdot\boldsymbol{n}] = 0. \tag{19}$$

The latter is zero since we assume no free charges.

Numerics

A second-order projection scheme is used to solve the Navier–Stokes equations. First, a temporary vector field, $\boldsymbol{a}$, is calculated:

$$\boldsymbol{a} = -(\boldsymbol{u}\cdot\nabla)\boldsymbol{u} + \nabla\cdot[\mu(\nabla\boldsymbol{u} + \nabla\boldsymbol{u}^T)]. \tag{20}$$

Then the pressure is found by solving

$$\nabla\cdot\left(\frac{\nabla p}{\rho}\right) = \nabla\cdot\boldsymbol{a}. \tag{21}$$

Finally, the velocity field is calculated with

$$\frac{\partial\boldsymbol{u}}{\partial t} = \boldsymbol{a} - \frac{\nabla p}{\rho} \tag{22}$$

The evolution in time is performed using a third order, strong stability preserving (SSP) Runge-Kutta (RK) method (Gottlieb *et al.* (2001)), while a second order SSP RK method is employed for the evolution of the level-set equation, the reinitialization of the level-set equation and extrapolation of the velocity field.

The equations are spatially discretized on a staggered grid, with scalar values stored in cell centers and vector values stored at cell boundaries. The convective terms are discretized using the fifth order Weighted Essentially Non-Oscillatory (WENO) scheme (Jiang and Peng (2000)), and viscous terms are discretized using standard second order central differences.

One substep in the RK solver can be summarized as follows:

1. Solve Equation (6) for the electric potential
2. Calculate electric field and electric forces using Equations (7)-(8)
3. Calculate a temporary vector field with Equation (20)
4. Solve Equation (21) to find the pressure
5. Calculate the final velocity field using Equation (22)
6. Extrapolate the velocity from the previous time step by solving Equation (11)
7. Update the level-set function with Equation (10), using the extrapolated velocities
8. Reinitialize the level-set function by solving Equation (13)

Dimensionless groups

In Yue *et al.* (2006) the following four dimensionless groups were used to describe the partial coalescence phenomena:
The Ohnesorge number, relating viscous forces to interfacial tension forces

$$Oh = \frac{\mu_1}{\sqrt{\rho_1 \sigma D}}, \tag{23}$$

the Bond number, relating gravitational forces to interfacial tension forces

$$Bo = \frac{|\rho_1 - \rho_2| g D^2}{\sigma}, \tag{24}$$

the density ratio

$$\rho^\star = \frac{\rho_1}{\rho_2} \tag{25}$$

and the viscosity ratio

$$\mu^\star = \frac{\mu_1}{\mu_2}. \tag{26}$$

Here, the subscripts 1 and 2 denote the drop and the matrix phase, respectively. D is the diameter of the drop and σ is the interfacial tension between the two phases. The addition of an electric field gives three new variables in the system; the initial electric field, E_0, and the permittivities of the two phases, ε_1 and ε_2. This calls for two new dimensionless variables to properly describe the system. Here, we choose the electric Bond number, relating electric forces to interfacial-tension forces

$$Be = \frac{\varepsilon_1 \varepsilon_0 D}{\sigma} E_0^2, \tag{27}$$

and the permittivity ratio

$$\varepsilon^\star = \frac{\varepsilon_1}{\varepsilon_2}. \tag{28}$$

Any other dimensionless quantity can now ideally be represented as a function of these dimensionless parameters.

We use the same time scale as Yue *et al.* (2006),

$$t_{\text{ic}} = \sqrt{\frac{\rho_1 D^3}{\sigma}}. \tag{29}$$

Quantity	Value
Initial drop diameter, D_0	1/3
Drop density, ρ_1	1.0
Drop viscosity, μ_1	1.0×10^{-2}
Drop permittivity, ε_1	180
Matrix density, ρ_2	1.0
Matrix viscosity, μ_2	1.0×10^{-2}
Matrix permittivity, ε_2	3
Interfacial tension, σ	1.0
Electric field, E_0	6.42×10^{4}

Table 1: Numerical parameters for the oscillating drop calculation.

CODE VALIDATION

Oscillating drop driven by an electric field

This test case aims at demonstrating the validity of the model for the electric forces. An initially spherical drop is exposed to an electric field. This will induce surface forces on the interface between the two fluids, set up by the permittivity difference, and result in a stretching of the drop in the direction of the electric field. This process is illustrated in Figure 1.

An expression for the steady-state elongation of the droplet can be found by balancing the hydrodynamic pressure with the electrostatic pressure (Garton and Krasucki (1964); Taylor (1964)). For drops with finite permittivities, this expression can be written as

$$E_0\sqrt{\frac{D_0\varepsilon_0\varepsilon_2}{\sigma}} = 2\left(\frac{a}{b}\right)^{2/3}\sqrt{2-\frac{b}{a}-\left(\frac{b}{a}\right)^3} \tag{30}$$

$$\cdot\left|\frac{1}{1-\varepsilon_1/\varepsilon_2}-\frac{b^2}{a^2}I_2\right| \tag{31}$$

$$I_2 = \frac{1}{2}e^{-3}\ln\left(\frac{1+e}{1-e}\right)-e^{-2} \tag{32}$$

$$e^2 = 1-\frac{b^2}{a^2} \tag{33}$$

$$\tag{34}$$

A series of calculations on varying grid sizes was performed and compared with the analytic expression above. The numerical parameters for the numerical calculations are given in Table 1. For these values, the asymptotic expression gives $a = 0.3290$ and $b = 0.3422$.

Figure 2 compares calculations with the axisymmetric code to the asymptotic value. As expected, the calculations converge toward oscillating around the asymptotic value.

Partial coalescence without electric field: Comparison with experiment

In Chen *et al.* (2006), an experiment was performed of a water droplet merging with an interface between 20 %

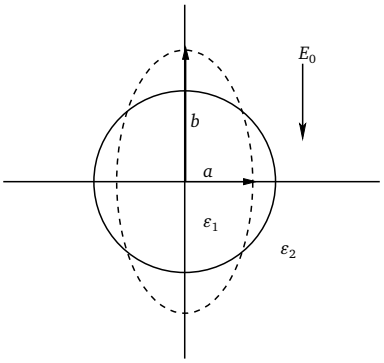

Figure 1: Illustration of the stretching of an initially spherical drop when an electric field is applied.

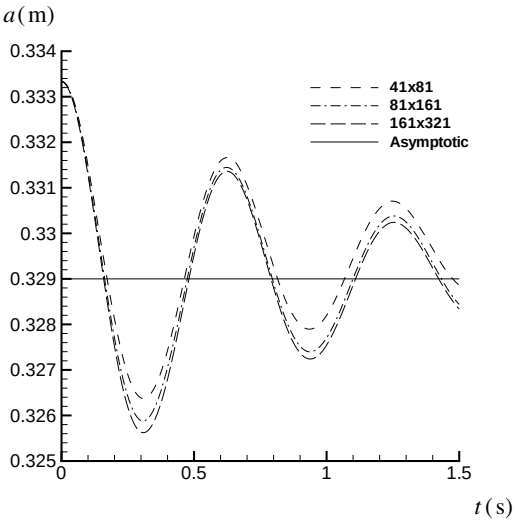

Figure 2: The evolution of the x-aligned semi-axis of an initially spherical drop subjected to an electric field. The dashed line indicates the theoretical steady state.

polybutene in decane and water, with no electric field applied. They presented a particularly clear image sequence of a partial coalescence event, which is used here for comparison with the numerical results. The physical properties of the system used are given in Table 2. Note that Chen *et al.* (2006) use a different definition of the Ohnesorge number than this work.

A numerical calculation with the same properties was performed to verify that the numerical method was capable of calculating the partial coalescence process. The numerical setup is illustrated in Figure 3. The computational domain is given by $R = 3D$ and $H = 6D$, the height of the water interface is $H_1 = 2D$ and the initial distance from the interface to the drop is $H_2 = 0.02D$. The grid size used was 100×200.

Figure 4 shows snapshots from the experiment performed in Chen *et al.* (2006), and Figure 5 shows the comparable snapshots from the numerical calculation. The simulation is capable of reproducing the partial coalescence of the experiment, and also captures the evolution of the interface with quantitative precision. In particular, the numerical method is capable of predicting the evolution of the capillary wave, indicated by arrows in Figure 4.

Quantity	Value
Drop diameter, D	1.1×10^{-3}
Drop density, ρ_1	1000
Drop viscosity, μ_1	1.0×10^{-3}
Matrix density, ρ_2	760
Matrix viscosity, μ_2	2.0×10^{-3}
Interfacial tension, σ	2.97×10^{-2}
Ohnesorge number, Oh	5.53×10^{-3}
Bond number, Bo	9.59×10^{-2}

Table 2: Physical properties of the partial coalescence experiment performed by Chen *et al.* (2006).

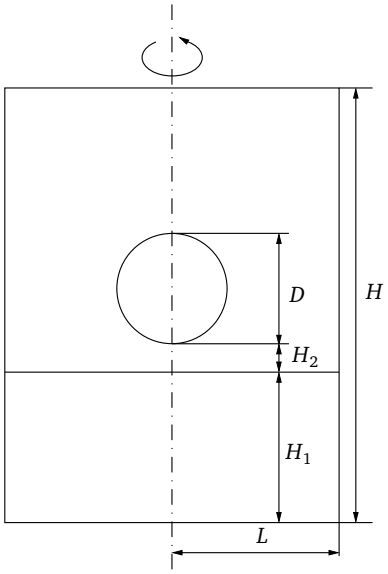

Figure 3: A schematic of the geometry for the numerical simulation. Axisymmetry is imposed across the centerline, so only the right half is actually part of the computational domain.

RESULTS AND DISCUSSIONS

In this section, the effect of an electric field on the partial coalescence process is discussed. Calculations are performed using the same numerical setup and physical properties as in the previous section, but now a potential difference is applied between the upper and lower boundary. Additionally, the height of the numerical domain is increased to $H = 7.5D$, to ensure that the drop is not affected by the upper boundary. The grid size used for these simulations was 90×225.

It should be noted that the initial conditions used here does not take into account the approach of the drop and the resting of the drop on the interface. Several authors (Charles and Mason (1960b); Allan and Mason (1961); Brown and Hanson (1965); Eow and Ghadiri (2003)) have found that an important effect of adding an electric field is a reduction in rest time due to additional attractive forces during the approach of the drop. However, the purpose of this study is to examine the actual coalescence process, and not the reduction in rest time.

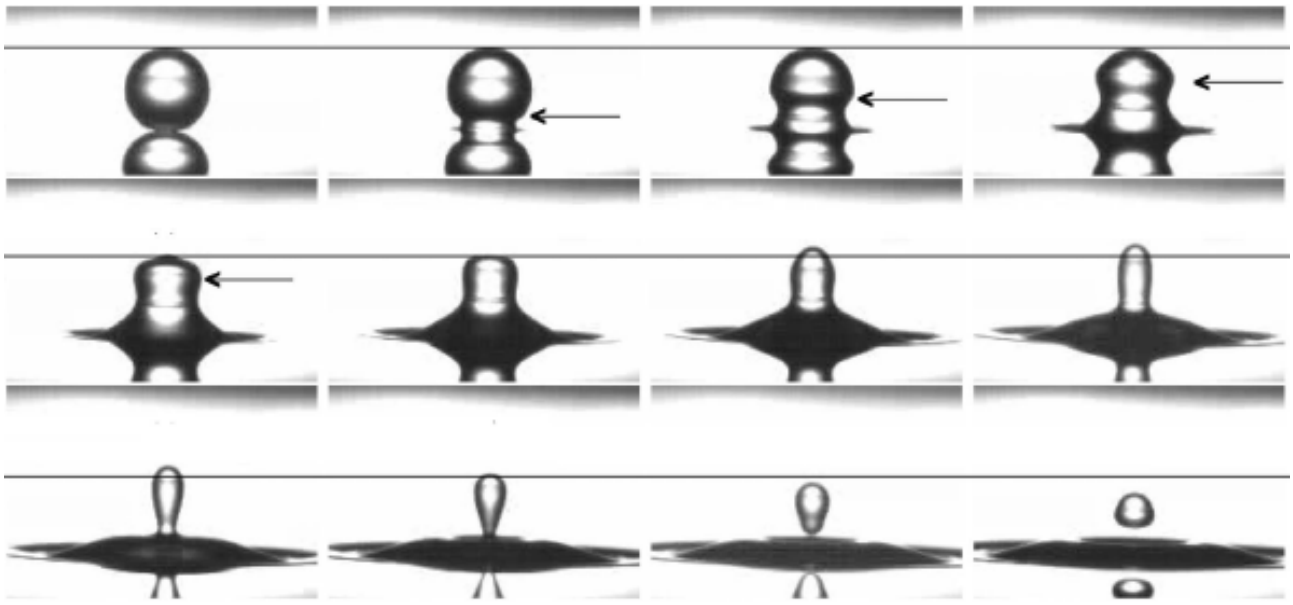

Figure 4: Snapshots of a water droplet merging with an interface between 20 % polybutene in decane and water. The initial drop diameter $D = 1.1\,\text{mm}, Bo = 0.0959, Oh = 0.00417$, and the pictures are $542\,\mu\text{s}$ apart in time. The location of the capillary wave is shown by the arrows. The horizontal lines, which are at the same height in all three rows, help in tracking the motion of the top of the drop. Reprinted with permission from X. Chen, S. Mandre and J. J. Feng, Partial coalescence between a drop and a liquid-liquid interface. *Phys. Fluids*, volume 18, 2006. Article 051705. Copyright 2006, American Institute of Physics.

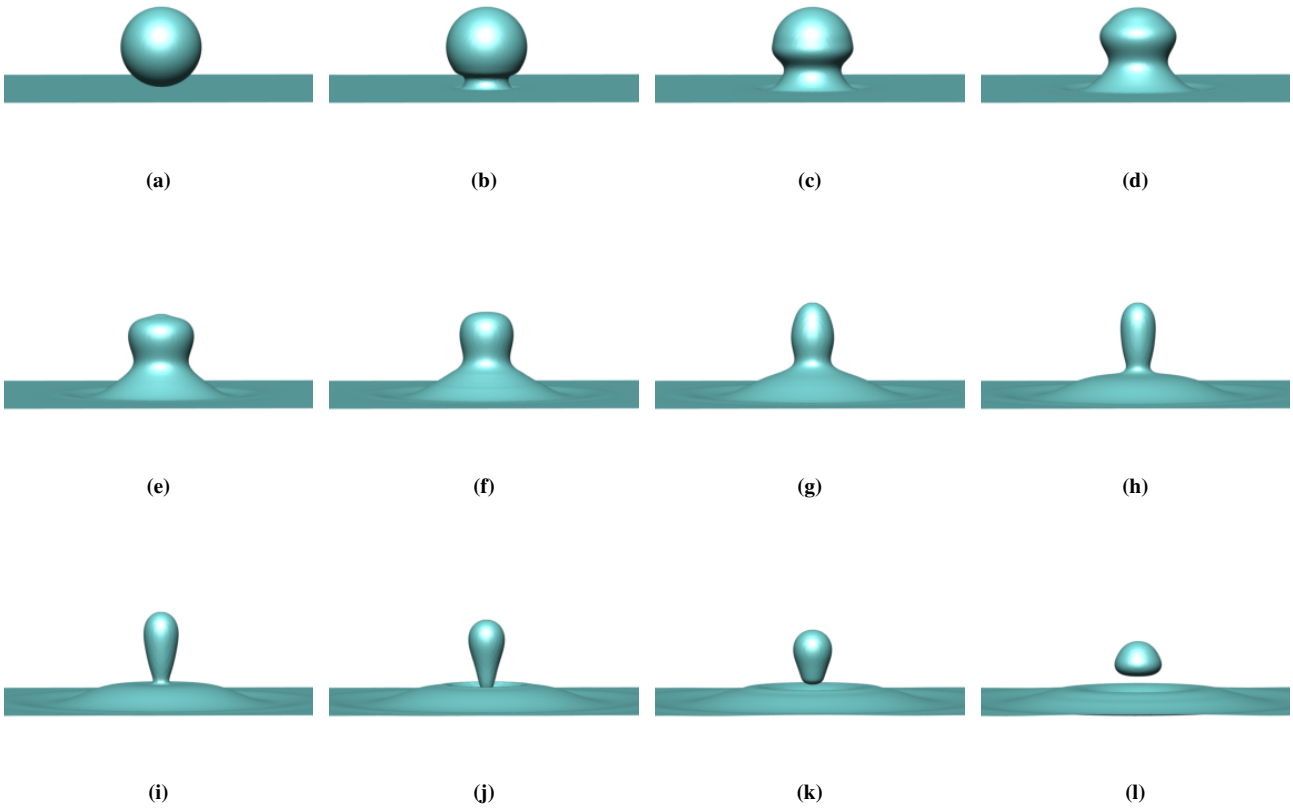

Figure 5: Snapshots from numerical simulation corresponding to the above figure. The numerical simulation is in good agreement with the experiment. In particular, the evolution of the capillary wave, indicated with arrows in the above figure, is accurately predicted.

Effect of the electric Bond number

Figure 6 shows the time interval from pinch-off to coalescence of the secondary drop, denoted τ_2, for different electric Bond numbers. The interval decreases until single stage coalescence is obtained at $Be = 0.075$. This trend is equivalent to that observed in Allan and Mason (1961). Single-staged coalescence is then observed at a range of electric Bond numbers, until pinch-off occurs again at $Be = 0.15$. The reappearance of multi-staged coalescence at higher field strengths was not observed by Allan and Mason (1961) and Eow and Ghadiri (2003). However, recent experiments (Hellesø (2008)) confirm that this behaviour may occur.

Snapshots from the entire calculation for $Be = 0.1$ are given in Figure 7. The potential drop across the drop and the aqueous phase is nearly zero, which was also observed in Allan and Mason (1961) and Brown and Hanson (1965). In Figure 4 it is clearly shown that without an electric field, the height of the liquid column increases during the emptying. With an electric field applied, the height decreases steadily throughout the entire event. The actual pinch-off in Figure 5, (k), corresponds to (h) in Figure 7. The liquid bridge for the simulation with an applied electric field is thicker, and the capillary forces are not large enough for pinch-off to occur.

Allan and Mason attributed single-stage coalescence to enhanced drainage of the drop due to electrostatic attraction. Figure 8 shows a comparison of the relative pressure distribution with and without an applied electric field at $t = 4.0 \times 10^{-4}$ s. The electric forces at the interface gives a higher pressure inside the drop, and hence a higher downward momentum. This is further illustrated in Figure 9, which shows the magnitude of the velocity in the y-direction. Without an electric field, the upper part of the liquid column has a positive velocity. Only the lower part of the column is emptied, which produces a thin filament which eventually pinches off. With an electric field, the entire column has a negative velocity, which additionally is everywhere larger than without an electric field. This increased emptying rate prevents the liquid bridge from pinching off. This also explains why the liquid bridge gets thinner from (b) to (h) in Figure 7, while it thickens thereafter. Initially, the capillary forces dominate, which causes a thinning of the liquid bridge. The capillary forces depend on the curvature, so they will get lower as the drop turns into a liquid column. Meanwhile, the pressure due to electric forces builds up inside the drop and accelerates the fluid inside. This is what causes the thickening and prevents pinch-off.

Effect of the permittivity ratio

Three simulations were performed at different permittivity ratios. The time from pinch-off to recoalescence is plotted in Figure 10. It is evident that for values much lower or higher than that used in the previous section, the coalescence becomes multi-staged again.

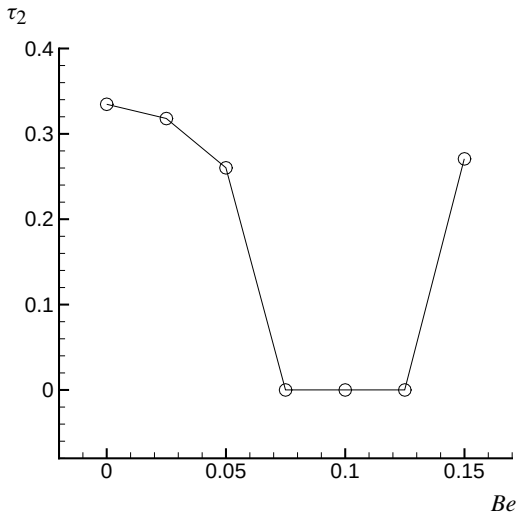

Figure 6: Time from pinch-off to recoalescence of secondary drop for varying electric Bond number. For an intermediate range of electric Bond numbers, the coalescence is single-staged.

For a low permittivity ratio, this is because the electric forces are too small to give the necessary downward momentum to prevent pinch-off.

For a high permittivity ratio, the increased stretching of the drop outweighs the effect of the downward momentum, which causes pinch-off to occur.

CONCLUSIONS

This article presented a computational investigation of the partial coalescence phenomenon, with and without electric fields applied.

It was shown that the numerical model is capable of reproducing a partial coalescence event with near quantitative precision in the absence of electric fields.

For the calculations with an applied electric field, the numerical model was able to reproduce trends reported in the literature. In particular, suppression of the partial coalescence process for higher electric fields observed in experiments was reproduced.

Detailed information from a single-staged coalescence event was presented that provides insight that is not immediately available from experiments. These results showed that the pressure inside the drop is higher when an electric field is applied. This increases the emptying rate of the drop, and thereby supports the argument that single-stage coalescence is caused by an increased downward momentum caused by the electric forces at the interface.

The present results do, however, not give a complete picture of partial coalescence under the influence of electric fields. More simulations should be performed using a wider range of the dimensionless parameters. In particular, only one Ohnesorge number and Bond number was investigated here. An investigation of higher Bond

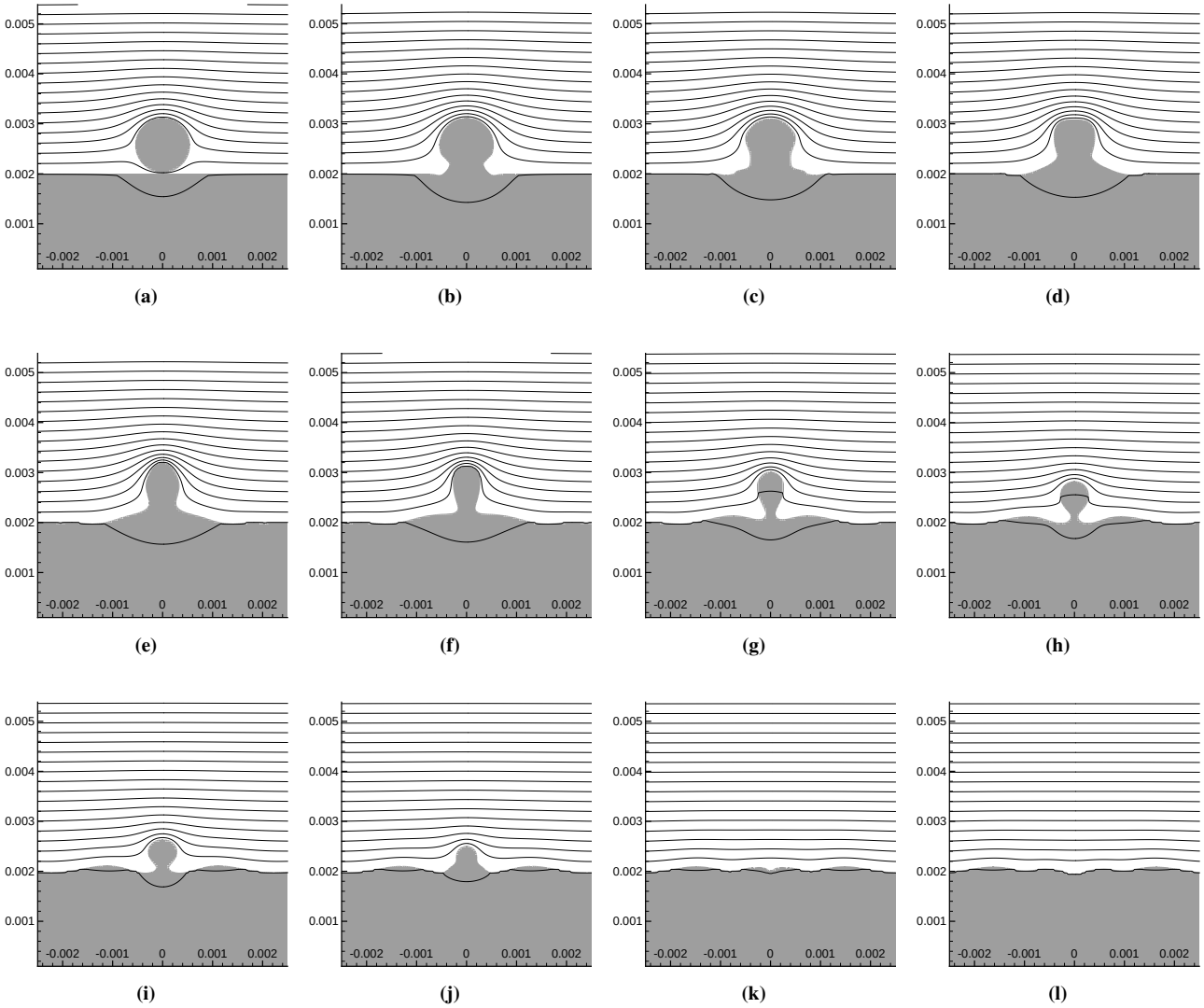

Figure 7: Snapshots from numerical simulation with $D = 1.1\,\text{mm}$, $Bo = 0.0959$, $Oh = 0.00417$, and $Be = 0.1$, demonstrating single stage coalescence. The time interval is $\Delta t = 7.75 \times 10^{-4}\,\text{s}$, and the contour lines show the electric potential with a 10 V interval. The potential in the aqueous phase is close to uniform, due to the high relative permittivity.

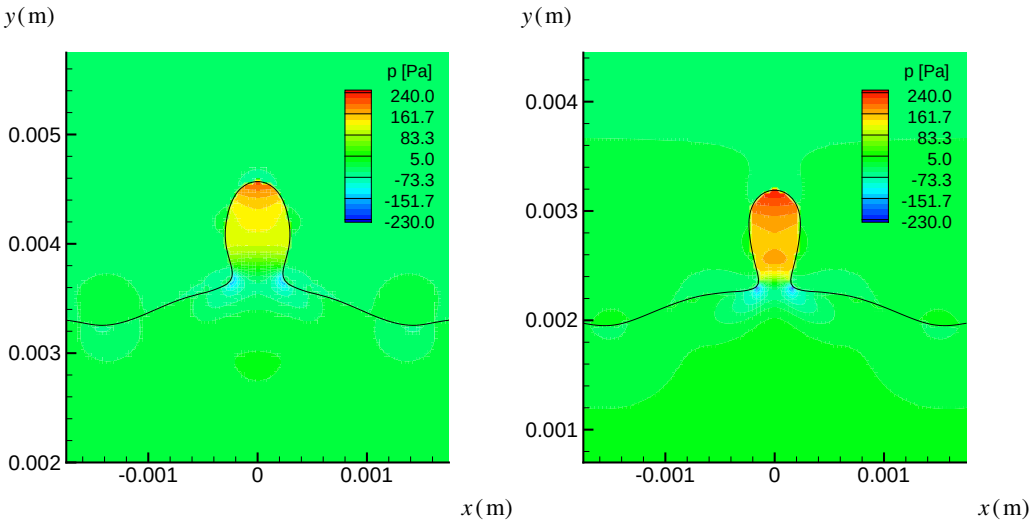

(a) No electric field

(b) Applied electric field, $Be = 0.1$

Figure 8: Contour plot of relative pressure at $t = 4.0 \times 10^{-4}\,\text{s}$, with and without an electric field. The electric field gives a higher pressure inside the drop, due to the additional electric forces at the interface.

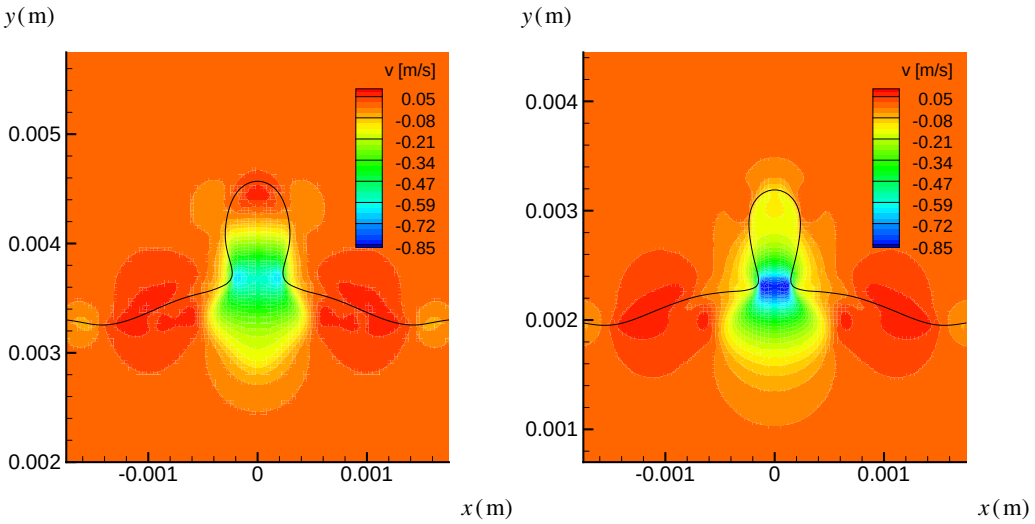

(a) No electric field

(b) Applied electric field, $Be = 0.1$

Figure 9: Contour plot of vertical velocity at $t = 4.0 \times 10^{-4}$ s, with and without an electric field. The electric field gives an increased emptying rate of the drop.

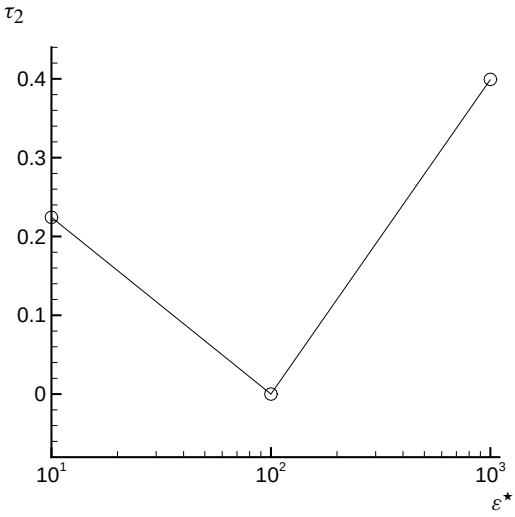

Figure 10: Time from pinch-off to recoalescence of secondary drop for varying permittivity ratio.

numbers, electric Bond numbers and permittivity ratios requires a full simulation of the approach of the drop.

Finally, the influence of impurities on the interface has not been taken into account in the numerical modeling. Such impurities may cause surface tension gradients which give rise to additional forces that may modify the coalescence behaviour. However, recent experiments (Hellesø (2008)) performed with water drops in real crude oils show the same qualitative behaviour as the results presented here.

ACKNOWLEDGEMENTS

This work is funded by the project "Electrocoalescence – Criteria for an efficient process in real crude oil systems"; co-ordinated by SINTEF Energy Research. The project is supported by The Research Council of Norway, under the contract no: 169466/S30, and by the following industrial partners: Aibel AS, Aker Kvaerner Process Systems AS, StatoilHydro ASA, BP Exploration Operating Company Ltd, Shell Technology Norway AS, Petrobras.

REFERENCES

Adalsteinsson, D. and Sethian, J. A. The fast construction of extension velocities in level set methods. *J. Comput. Phys.*, volume 148: pages 2–22, 1999.

Allan, R. S. and Mason, S. G. Effects of electric ifelds on coalescence in liquid+liquid systems. *Trans. Faraday Soc.*, volume 57: pages 2027–2040, 1961.

Bjørklund, E. The level-set method applied to droplet dynamics in the presence of an electric field. *Comput. Fluids*, 2008. Accepted.

Blanchette, F. and Bigioni, T. P. Partial coalescence of drops at liquid interfaces. *Nat. Phys*, volume 2, no. 254, 2006.

Brown, A. H. and Hanson, C. Effect of oscillating electric fields on coalescence in liquid+liquid systems. *Trans. Faraday Soc.*, volume 61: pages 1754–1760, 1965.

Charles, G. E. and Mason, S. G. The coalescence of liquid drops with flat liquid/liquid interfaces. *J. Colloid Sci.*, volume 15: pages 236–267, 1960a.

Charles, G. E. and Mason, S. G. The mechanism of partial coalescence of liquid drops at liquid/liquid interfaces. *J. Colloid Sci.*, volume 15: pages 105–122, 1960b.

Chen, X., Mandre, S. and Feng, J. J. Partial coalescence between a drop and a liquid-liquid interface. *Phys. Fluids*, volume 18, no. 051705, 2006.

Eow, J. S. and Ghadiri, M. The behaviour of a liquid-liquid interface and drop-interface coalescence under the influence of an electric field. *Colloids and Surfaces*

A: Physiochem. Eng. Aspects, volume 215: pages 101–123, 2003.

Fedkiw, R. P. A non-oscillatory eulerian approach to interfaces in multimaterial flows. *J. Comput. Phys.*, volume 152: pages 457–492, 1999.

Garton, C. G. and Krasucki, Z. Bubbles in insulating liquids: Stability in an electric field. *Proc. R. Soc. London*, volume 280: pages 221–226, 1964.

Gilet, T., Mulleners, K., Lecomte, J. P., Vandewalle, N. and Dorbolo, S. Critical parameters for the partial coalescence of a droplet. *Phys. Rev. E*, volume 75, no. 036303, 2007.

Gottlieb, S., Shu, C. W. and Tadmor, E. Strong stability-preserving high-order time discretization methods. *SIAM Review*, volume 43: pages 89–112, 2001.

Hansen, E. B. *Numerical simulation of droplet dynamics in the presence of an electric field*. Ph.D. thesis, NTNU, 2005.

Hellesø, S. M. Personal communication, 2008.

Jiang, G. S. and Peng, D. Weighted eno schemes for hamilton-jacobi equations. *SIAM J. Sci. Comp.*, volume 21: pages 2126–2143, 2000.

Kang, M., Fedkiw, R. and Liu, X. A boundary condition capturing method for multiphase incompressible flow. *J. Sci. Comput.*, volume 15: pages 323–360, 2000.

Osher, S. and Fedkiw, R. *Level set methods and dynamic implicit surfaces*. Springer, 2003.

Sussman, M., Smereka, P. and Osher, S. A level set approach for computing solutions to incompressible two-phase flow. *J. Comput. Phys.*, volume 114: pages 146–159, 1994.

Taylor, G. Disintegration of water droplets in an electric field. *Proc. R. Soc. London*, volume 280: pages 383–397, 1964.

Thoroddsen, S. T. and Takehara, K. The coalescence cascade of a drop. *Phys. Fluids*, volume 12, no. 1265, 2000.

Yue, P., Zhou, C. and Feng, J. J. A computational study of the boalescence between a drop and an interface in newtonian and viscoelastic fluids. *Phys. Fluids*, volume 18, no. 102102, 2006.